Journal of the Korean Magnetic Resonance Society **2013**, *17,* 11-18
DOI 10.6564/JKMRS.2013.17.1.011

Effects of generalized-Born implicit solvent models in NMR structure refinement

Jun-Goo Jee*

Research Institute of Pharmaceutical Sciences, College of Pharmacy, Kyungpook National University, 80 Daehak-ro, Buk-gu, Daegu 702-701, Republic of Korea

Received May 13, 2013; Revised June 04, 2013; Accepted June 10, 2013

Abstract Rapid advances of computational power and method have made it practical to apply the time-consuming calculations with all-atom force fields and sophisticated potential energies into refining NMR structure. Added to the all-atom force field, generalized-Born implicit solvent model (GBIS) contributes substantially to improving the qualities of the resulting NMR structures. GBIS approximates the effects that explicit solvents bring about even with fairly reduced computational times. Although GBIS is employed in the final stage of NMR structure calculation with experimental restraints, the effects by GBIS on structures have been reported notable. However, the detailed effect is little studied in a quantitative way. In this study, we report GBIS refinements of ubiquitin and GB1 structures by six GBIS models of AMBER package with experimental distance and backbone torsion angle restraints. Of GBIS models tested, the calculations with igb=7 option generated the closest structures to those determined by X-ray both in ubiquitin and GB1 from the viewpoints of root-mean-square deviations. Those with igb=5 yielded the second best results. Our data suggest that the degrees of improvements vary under different GBIS models and the proper selection of GBIS model can lead to better results.

Keywords NMR, all-atom force field, generalized-Born implict solvent model

Introduction

Conventional 3D structure determination of a biomolecule by experimental NMR restraints is an iterative process in which the structure calculation is tightly coupled with the assignment of NOE distance restraints[1]. Advances in NOE assignment and calculation algorithms have enabled the automatic calculation of protein 3D structures only with NOESY data, provided chemical shifts are assigned in most atoms and sufficient NOE peaks exist[2]. Accompanying rapid advances in calculation capacity, recent studies have reported that full automatic structure calculations with the raw data even without any manual interpretation are feasible[3, 4]. However, the improvements and refinements of NMR structures have been thought mainly dependent on the skills and experiences of the researchers who interpret and analyze the data.

Despite the sensitivity increments by updated NMR hardware and the developments of new experiments for the last decades, the number of experimentally obtainable NMR restraints for determining a 3D structure is much smaller compared with that used in X-ray crystallography. Computational aids have contributed to overcoming the lack of restraints and improving structural qualities of NMR structures. The endeavors can be classified into two criteria — the use of empirical information from 3D structure database and the application of state-of-the-art calculation methods that have become mature for molecular dynamics (MD) simulation. The main improvements through the calculation methods stem from the realistic force field consisting of all-atom force field and generalized-Born implicit solvent

* Address correspondence to: **Jun-Goo JEE,** Research Institute of Pharmaceutical Sciences, College of Pharmacy, Kyungpook National University, 80 Daehak-ro, Buk-gu, Daegu 702-701, Republic of Korea; E-mail: jjee@knu.ac.kr

model (hereafter GBIS)[5]. All-atom force field employs sophisticated energy terms including Lennard-Jones potential, which locate atoms more optimal positions. GBIS moreover enables to approximate solvation effects with comparably reduced computational times than handling solvents explicitly.

We have demonstrated the usefulness of GBIS by improving the qualities of NMR structures in a series of protein-protein complexes. Due to the transient features of the interface in protein-protein complex, it is often not straightforward to obtain sufficient distance restraints to fix the relative orientations of two proteins. GBIS has helped to refine the interfacial geometries in the cases of UIM-ubiquitin[6,7] $GB1^{A34F}$ dimer[8], UBA-ubiquitin[9], UIM-K63-diubiquitin[10], and VAP^{MMP}-$OBSP^{FFAT}$ complexes[11]. Our extended research have also shown that GBIS could determine an intermolecular hydrogen bond unambiguously in UIM and ubiquitin complex, which is difficult to be observed by other experimental methods[6] Another example that demonstrated the performance of GBIS was the refinement of a protein structure where NMR signals were measured under membrane-like environments. By using an optimized surface tension coefficient for the hydrophobic surroundings, we could improve NMR structures to have closer solvent accessible surface areas to those of X-ray structure[12].

Considering the potentials of GBIS, which have been reflected by our accumulated results, the applications for NMR structure refinement will increase. However, comparison of resulting NMR structures under different GBIS models is little known. Because GBIS still needs considerable computational times, there is a need to know the optimal parameters a priori for the end users. We in this study have performed NMR structure refinements with the proteins of ubiquitin and GB1 by GBIS models. We tested total six GBIS models under experimentally obtained distance and torsion angle restraints with AMBER package (ver. 12) [13].

Experimental Methods

We first calculated 300 structures of ubiquitin and GB1 with experimental distance and torsion angle restraints by using CYANA[14]. The top 100 structures that did not show significant violations against experimental inputs were chosen. Here 20,000 steps of torsion angle dynamics were employed. We refined the 100 structures with GBIS models of AMBER package. The AMBER calculation with GBIS models consisted of three stages — 1,500 steps of energy minimization, 20 ps molecular dynamics (MD), and 1,500 steps of energy minimization. As a conformational search method during MD simulation, we applied a restrained simulated annealing with PMEMD or SANDER module of AMBER package. Here the temperature was increased to 1,000 K for the first 10 ps, followed by a stepwise cooling stage to 0 K for the second 10 ps. The experimental restraints for the structure calculations of ubiquitin and GB1 were extracted from those deposited as PDB IDs of 1D3Z and 3GB1 in the PDB database (http://www.rcsb.org), respectively. Only the restraints from NOE-derived distance as well as backbone torsion angle were employed. The numbers of distance restraints were 1,446 and 584 for ubiquitin and GB1, respectively. In detail, the distance restraints for ubiquitin (GB1) consisted of 288(122), 294(122), 236(83), and 628(257) for intra ($|i-j|=0$), sequential ($|i-j|=1$), medium ($1<|i-j|<5$), and long ($|i-j|>4$) range ones, respectively. The torsion angle restraints comprised 62 angles for ubiquitin, whereas those for phi and psi in GB1 were 52 and 49. The force constants for distance and torsion-angle restraints were 50 $kcal \cdot mol^{-1} \cdot Å^{-2}$ and 200 $kcal \cdot mol^{-1} \cdot rad^{-2}$, respectively. Of 100 structures, the best 20 structures showing the lowest energies and no significant violations against distance and torsion angle restraints were selected as an ensemble for further analyses. All the calculations were performed with in-house built Mac-mini cluster machines consisting of 80 cores in total. AMBER (ver. 12) has six GB models available, which are executed by the options of igb=1,2,5,6,7,8. All the calculations were performed under ff99SB force field. For quantitative analyses, in addition to AMBER energy, the resulting structures were compared from the viewpoints of two

RMSDs — one between resulting structures and the other between resulting structures (eRMSD; ensemble root mean square deviation) and reference X-ray structures (bRMSD; biased root mean square deviation), 1UBQ for ubiquitin and 2QMT for GB1, repectively. We also included two well refined NMR structures of ubiquitin (1D3Z) and GB1 (3GB1) that were calculated with extensive experimental restraints including residual dipolar coupling and J-coupling constants for comparison. As other parameters for analyses, we calculated the percentage of most favored region at Ramachandran plot[15], the number of hydrogen bonds, and the MolProbity packing scores[16]. These parameters were calculated by PROCHECK-NMR, MOLMOL[17], and MolProbity software packages, respectively.

Results

GBIS refinements improved structures in terms of both precision and accuracy- All the results including statistical analyses were listed in Table-1~4 along with GB models in use. For a fair comparison, we chose top 20 of 100 CYANA structures. All the structures by GBIS refinement represented significant improvements in the precision, which was revealed by eRMSD (ensemble RMSD in backbone/side-chain atoms), compared with those by CYANA. Also the accuracy — which is roughly shown by bRMSD (biased RMSD between backbone atoms) and the portion of most favored region in Ramachandran analyses — increased considerably. The degrees of improvements were similar to those found in our previous results[6, 12]. One may argue on the largeness of bRMSD values. Indeed, bRMSD had the values of 0.8 ~ 1.0 Å, which were greater than eRMSD (0.3 ~ 0.4 Å), suggesting that structural disagreements might exist. It should be noted, however, that the dissimilarities were pre-existing in the template CYANA structures — 1.06 and 1.00 Å bRMSD against ubiquitin and GB1 X-ray ones, respectively. Thus GBIS did force nearly all the refined structures move closer to X-ray and NMR structures. Nevertheless it would be inadequate to directly compare the structures by CYANA and GBIS, because the force field of CYANA is simplified and optimized for calculation speed.

GBIS model of igb=7 generated the best results in the viewpoints of backbone RMSD- The best degree of improvement in bRMSD − from 1.06 to 0.86 Å in ubiquitin and from 1.00 to 0.80 Å in GB1 − toward X-ray structures were found in the results with igb=7, both in ubiquitin and GB1 cases. The improvement of 0.2 Å in bRMSD is significant, since the value is more than two times greater than standard deviation of 0.09 Å in eRMSD. Visual inspection exhibited the tendencies as well. When the structures by igb=7 were overlaid with X-ray and NMR structures, the regions that were not overlaid mainly located at loops (Fig. 1). The lacks of experimental restraints in the region may have enabled GBIS to relocate the parts to have energetically more favorable geometries. It is noteworthy again that there was no significant violation in the resulting ensemble structures against input experiments restraints despite the changes of structures.

GBIS model of igb=7 generated the best results in in the viewpoints of side-chain packing as well- The simple comparisons of backbone geometries by using torsion angles of psi and psi between structures did not reveal clearly how much the resulting structures improved (data not shown). The observation that the portions of the most favored regions at Ramachandran plots were all comparable in GBIS results could reflect the indistinguishability in the qualities of backbone geometries. In order to clarify the improvements via GBIS refinement, we instead quantified the geometrical qualities of side-chains by using MolProbity. MolProbity generates two overall parameters of Clash score (C-score) and MolProbity score (M-score), which reflect the qualities of all-atom contacts and protein geometries, respectively. In both scores, the lower values indicate the better qualities. For instance, 0.0 implies the best structure at 100 percentile, while 1.42 and 1.53 correspond to 95.8 and 93.8 percentiles in M-score, respectively. Whereas all the structures by GBIS

Table 1. GBIS refined ubiquitin structures*
*The values following the mean values with ± in all the tables indicate standard deviation (SD).
**"n.a." means "not available".

Model	eRMSD (Å) Backbone All-atoms	bRMSD (Å) Backbone	Amber Energy (kcal/mol)	Most favored region of Ramachandran analysis (%)	Clash score MolProbity score	Number of H-bonds All (bb/sc)
PDB(X-ray)	n.a.**	0	n.a.	95.5	8.430 2.174	55 (40/15)
PDB(NMR)	0.09 ± 0.02 0.55 ± 0.06	0.37 ± 0.02	n.a.	96.7	5.064 ± 1.380 1.308 ± 0.115	44 (40/4)
CYANA	0.41 ± 0.05 0.82 ± 0.07	1.06 ± 0.09	n.a.	72.9	0.486 ± 0.407 2.234 ± 0.184	9 (9/0)
igb=1	0.31 ± 0.04 0.76 ± 0.06	0.94 ± 0.05	-2,613 ± 10	87.3	0.365 ± 0.413 1.528 ± 0.168	38 (31/7)
igb=2	0.29 ± 0.04 0.76 ± 0.05	0.91 ± 0.04	-2,633 ± 10	87.6	0.203 ± 0.360 1.404 ± 0.176	36 (31/5)
igb=5	0.29 ± 0.05 0.74 ± 0.06	0.88 ± 0.05	-2,523 ± 10	88.9	0.122 ± 0.297 1.386 ± 0.115	40 (34/6)
igb=6	0.33 ± 0.06 0.79 ± 0.06	0.94 ± 0.05	-2,613 ± 11	87.3	0.203 ± 0.360 1.430 ± 0.225	35 (31/4)
igb=7	0.25 ± 0.04 0.67 ± 0.05	0.86 ± 0.04	-2,625 ± 9	86.7	0.041 ± 0.181 1.416 ± 0.185	41 (35/6)
igb=8	0.30 ± 0.05 0.73 ± 0.03	0.92 ± 0.04	-2,686 ± 10	87.3	0.365 ± 0.413 1.528 ± 0.168	40 (34/6)

Table 2. GBIS refined GB1 structures

Model	eRMSD (Å) Backbone All-atoms	rRMSD (Å)	Amber Energy (kcal/mol)	Most favored region of Ramachandran analysis (%)	Clash score MolProbity score	Number of H-bonds All (bb/sc)
PDB(X-ray)	n.a.	0	n.a.	96.0	4.360 1.834	46 (34/12)
PDB(NMR)	0.23 ± 0.04 0.71 ± 0.08	0.70 ± 0.04	n.a.	94.4	10.236 ± 3.399 1.785 ± 0.247	27 (26/1)
CYANA	0.39 ± 0.11 0.89 ± 0.12	1.00 ± 0.09	n.a.	86.9	0.000 ± 0.000 1.790 ± 0.140	16 (16/0)
igb=1	0.38 ± 0.08 0.90 ± 0.07	0.83 ± 0.14	-1,633 ± 9	94.1	0.000 ± 0.000 1.319 ± 0.259	33 (30/3)
igb=2	0.39 ± 0.08 0.86 ± 0.07	0.84 ± 0.12	-1,646 ± 8	94.1	0.000 ± 0.000 1.264 ± 0.203	31 (29/2)
igb=5	0.36 ± 0.07 0.84 ± 0.06	0.90 ± 0.12	-1,590 ± 8	92.9	0.058 ± 0.262 1.339 ± 0.204	34 (31/3)
igb=6	0.23 ± 0.05 0.56 ± 0.05	1.00 ± 0.08	-1,006 ± 13	93.2	2.106 ± 1.046 1.719 ± 0.245	37 (30/5)
igb=7	0.34 ± 0.07 0.79 ± 0.07	0.80 ± 0.08	-1,637 ± 7	90.0	0.000 ± 0.000 1.271 ± 0.220	33 (31/2)
igb=8	0.38 ± 0.11 0.85 ± 0.10	0.84 ± 0.10	-1,677 ± 7	91.9	0.000 ± 0.000 1.247 ± 0.236	36 (33/3)

Table 3. χ_1-angle statistics of ubiquitin structures[***]
[***]All the values indicate degrees.

Model	Phe-4	Phe-45	Tyr-59	His-68
PDB(X-ray)	-60.7	178.0	-63.3	-69.1
PDB(NMR)	-62.2 ± 1.2	175.5 ± 2.1	-68.6 ± 2.0	-67.5 ± 1.5
CYANA	58.7 ± 15.5	175.5 ± 6.2	-82.2 ± 7.9	-72.7 ± 15.2
igb=1	-72.7 ± 4.1	164.7 ± 2.8	-74.9 ± 2.3	-47.0 ± 20.7
igb=2	-72.9 ± 3.0	166.9 ± 4.8	-76.4 ± 2.8	-46.3 ± 19.9
igb=5	-73.2 ± 2.8	166.2 ± 4.5	-76.9 ± 4.2	-43.8 ± 2.9
igb=6	-73.6 ± 3.8	165.0 ± 4.3	-74.8 ± 2.7	-45.0 ± 19.8
igb=7	-71.3 ± 2.4	167.2 ± 4.3	-73.6 ± 2.0	-56.8 ± 4.6
igb=8	-74.8 ± 19.5	167.3 ± 5.5	-74.3 ± 2.5	-61.7 ± 6.7

Table 4. χ_1-angle statistics of GB1 structures

Model	Tyr-3	Phe-30	Tyr-33	Trp-43	Tyr-45	Phe-52
PDB(X-ray)	-66.0	-71.2	167.5	-73.0	173.4	-64.4
PDB(NMR)	-66.8 ± 2.5	-75.2 ± 2.6	-179.4 ± 2.1	-73.9 ± 1.7	171.0 ± 1.4	-77.6 ± 2.1
CYANA	-56.1 ± 4.0	-75.0 ± 2.4	177.5 ± 3.1	-70.3 ± 3.9	173.9 ± 1.1	-100.1 ± 4.0
igb=1	-62.6 ± 2.8	-74.4 ± 1.3	168.1 ± 2.1	-71.4 ± 3.0	166.1 ± 1.9	-73.2 ± 2.3
igb=2	-61.9 ± 3.2	-73.9 ± 1.2	168.7 ± 2.3	-70.0 ± 1.4	165.8 ± 1.4	-73.6 ± 2.5
igb=5	-64.5 ± 3.3	-73.3 ± 1.0	168.5 ± 1.9	-70.8 ± 1.8	165.7 ± 1.3	-72.7 ± 2.5
igb=6	-62.5 ± 5.6	-73.0 ± 1.2	169.8 ± 1.6	-76.5 ± 1.5	168.6 ± 1.9	-80.7 ± 1.9
igb=7	-63.2 ± 2.8	-72.7 ± 1.0	169.4 ± 1.3	-68.4 ± 1.1	167.2 ± 1.5	-73.1 ± 1.8
igb=8	-61.9 ± 3.0	-73.6 ± 0.8	168.4 ± 1.5	-70.4 ± 1.4	167.2 ± 1.6	-72.4 ± 2.5

showed the comparable M-scores, there were large varieties in C-scores. Here again the structures with GBIS of igb=7 revealed the lowest values in both proteins. The value of 0.041 by igb=7, which corresponds to almost 100 percentile, was the smallest among all M-scores in ubiquitin case. On the

other hand, all the refined structures of GB1 showed the perfect C-scores around 0, meaning that all-atoms were located with ideal clashes in the structures.

Number of hydrogen bonds- It has been reported that GBIS refinement increases the number of hydrogen bonds (5). Some modeling programs that include the energy terms derived from hydrogen bond geometries improved structural qualities. Since AMBER force field does not employ the energy term accounting for hydrogen bond, the increment of hydrogen bonds may adequately reflect the qualities of structures. We judged that there is a hydrogen bond when more than 15 of 20 structures in an ensemble contain the same hydrogen bond. All the NMR structures revealed the smaller number of hydrogen bonds than X-ray structure. Nevertheless GBIS increased the numbers remarkably, particularly in the cases of side-chains (Table-1 & 2). The structures by igb=7 revealed the highest number of backbone hydrogen bonds, followed by igb=5 and igb=8 in ubiquitin. The order was igb=8, igb=5, and igb=7 in GB1. Because the variation in numbers was subtle, we could not extract the direct relationship between the number of hydrogen bonds and the other parameters. Nonetheless, the tendency that the more qualified structures revealed more hydrogen bonds was clear.

Precision and accuracy of aromatic side-chains- In order to further understand the structural differences, we investigated the conformation of aromatic side-chains by inspecting $\chi 1$-angles. The conformation of an aromatic side-chain is a good indicator reflecting the accuracy and precision of NMR structure ensemble. Due to the practical difficulty of obtaining distance restraints from aromatic regions directly, the parts in an ensemble are often divergent, even leading to wrong $\chi 1$-angle geometries (12). Ubiquitin constains 4 aromatic residues (Phe-4, Phe-45, Tyr-59, and His-68), whereas GB1 has 6 (Tyr-3, Phe-30, Tyr-33, Trp-43, Tyr-45, and Phe-52). The overlaid figures of aromatic regions demonstrated the robustness of GBIS method convincingly (Fig. 1). Even though we did not include $\chi 1$-angle information as restraints, the most of refined structures had well converged geometries, not deviating much ($\pm$ 30 degrees) from the values of 1 -angle in X-ray structures. It should be noted that GBIS could relocate the wrong $\chi 1$-angle of ubiquitin Phe-4 in CYANA structure (58.7°) to have correct geometries (71.3° for igb=7). Overall convergences of the aromatic side-chains improved as well, including the surface exposed His-68 in ubiquitin. The regions around His-68 are important for recognizing ubiquitin interacting motifs[7]. Therefore, the precise $\chi 1$ geometry that was reflected by smaller standard deviation value ($\pm$ 4.6° for igb=7) would probably be beneficial for the better understanding of the function.

Discussion

The improvements that are reflected by the values of eRMSD, bRMSD, C-Score, M-score, the number of hydrogen bonds, and $\chi 1$-angles indicate unambiguously that GBIS refinement did improve the qualities of starting structures without violating input experimental restraints. Our results, therefore, again recommend the employment of GBIS in refining NMR structures. Then, which GBIS model would be the most recommendable? Our data showed that igb=7 yielded the best results in general, followed by igb=5, at least in the two cases of ubiquitin and GB1. One may argue that the improvements in the resulting structures by different models were less significant. However, the conformational spaces that GBIS would forces were limited under the current experimental restraints. It should be noted that we employed the PDB-deposited distance and backbone torsion angle restraints for GBIS refinement. And the numbers — 1,446 and 584 distance restraints for ubiquitin and GB1, respectively — are regarded sufficient for NMR structure determination. Small degree of improvements, in addition, may provide a comprehensive explanation for unanswered functions. For instance, aromatic residues exposed on protein surface are usually important for the recognition of

ligands or proteins, and the correct geometry may offer a valuable clue to predict and understand the function[7, 18]. If one can achieve measurable improvement by investing the same computational time, it will be advantageous.

Computational capacity has been dramatically growing along with the advents of new hardware such as NVIDIA GPU (Graphic Processing Unit) and Intel MIC (Many Integrated Core). Use of more sophisticated calculation methods than GBIS will become practical in near future, which includes the refinement with explicit solvents. It will in turn increase the needs to know the pros and cons between implicit and explicit solvents in refining NMR structures. Our current data will be a meaningful addition for the purpose.

The GBIS model of igb=7 uses a pairwise correction term to igb=1 (GB^{HCT} model), to approximate a molecular surface dielectric boundary to eliminate interstitial regions of high dielectric smaller than a solvent molecule[19]. Different from igb=2 (GB^{OBC} model) which uses geometry-free average re-scaling approach, however, the correction by igb=7 affects all atoms and is geometry-specific. In this study, we did not discuss on the mathematical details and differences of each GB models, but focused on the practical uses, by inspecting the resulting structures. There will be plenty of combinations between force fields and GB models to test. Understanding theoretical details may give us more comprehensive information. Also knowing how much several GBIS models generate different results under a variety of experimental restraints will be informative. We will address on these issues elsewhere. The well-refined

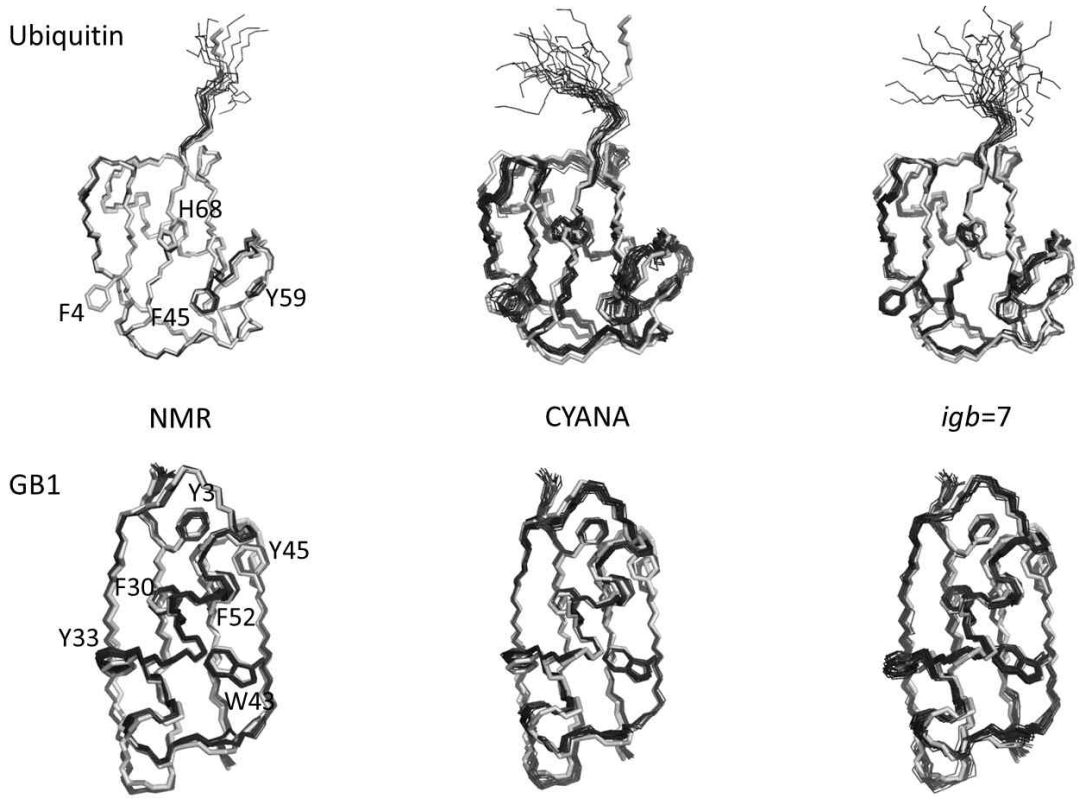

Figure 1. Visual comparison of structures. Overlaid ensembles in deposited-NMR, CYANA, and GBIS-refined (igb=7) structures. Ensemble structures are drawn in black, whereas X-ray structure in gray. Aromatic side-chains are shown and labeled for comparison. The figures were generated by MOLMOL [17].

3D coordinate by GBIS can be coupled with pharmaceutical applications such as structure-based ligand discovery[20]. We will discuss the results elsewhere as well.

In conclusion, our current results have provided practical information in employing GBIS to NMR structure determination of protein. It will be helpful particularly for the proteins that are biologically important but difficult to determine the structures with conventional NMR approaches [21].

Acknowledgement

This Research was supported by Kyungpook National University Research Fund, 2011, to the author.

References

1. Wüthrich, K. *NMR of Proteins and Nucleic Acids*; Wiley: New York, (1986).
2. Herrmann, T.; Güntert, P.; Wüthrich, K. *Journal of molecular biology.* **319**, 209. (2002).
3. Schmidt, E.; Güntert, P. *Journal of the American Chemical Society*. **134**, 12817. (2012).
4. Lopez-Mendez, B.; Güntert, P. *Journal of the American Chemical Society*. **128**, 13112. (2006).
5. Xia, B.; Tsui, V.; Case, D. A.; Dyson, H. J.; Wright, P. E. *Journal of biomolecular NMR*. **22**, 317. (2002).
6. Jee, J. *Bull Korean Chem Soc.* **31**, 2717. (2010).
7. Fujiwara, K.; Tenno, T.; Sugasawa, K.; Jee, J. G.; Ohki, I.; Kojima, C.; Tochio, H.; Hiroaki, H.; Hanaoka, F.; Shirakawa, M. *The Journal of biological chemistry.* **279**, 4760. (2004).
8. Jee, J.; Byeon, I. J.; Louis, J. M.; Gronenborn, A. M. *Proteins* .**71**, 1420. (2008).
9. Ohno, A.; Jee, J.; Fujiwara, K.; Tenno, T.; Goda, N.; Tochio, H.; Kobayashi, H.; Hiroaki, H.; Shirakawa, M. *Structure* **13**, 521. (2005).
10. Sekiyama, N.; Jee, J.; Isogai, S.; Akagi, K.; Huang, T. H.; Ariyoshi, M.; Tochio, H.; Shirakawa, M. *Journal of biomolecular NMR.* **52**, 339. (2012).
11. Furuita, K.; Jee, J.; Fukada, H.; Mishima, M.; Kojima, C. *The Journal of biological chemistry.* **285**, 12961. (2010).
12. Jee, J.; Ahn, H. C. *Bull Korean Chem Soc.* **30**, 1139. (2009).
13. Case, D. A.; Cheatham, T. E., 3rd; Darden, T.; Gohlke, H.; Luo, R.; Merz, K. M., Jr.; Onufriev, A.; Simmerling, C.; Wang, B.; Woods, R. J. *J Comput Chem.* **26**, 1668. (2005).
14. Güntert, P.; Mumenthaler, C.; Wüthrich, K. *Journal of molecular biology.* **273**, 283. (1997).
15. Laskowski, R. A.; Rullmannn, J. A.; MacArthur, M. W.; Kaptein, R.; Thornton, J. M. *Journal of biomolecular NMR.* **8**, 477. (1996).
16. Davis, I. W.; Leaver-Fay, A.; Chen, V. B.; Block, J. N.; Kapral, G. J.; Wang, X.; Murray, L. W.; Arendall, W. B., 3rd; Snoeyink, J.; Richardson, J. S.; Richardson, D. C. *Nucleic acids research.* **35**, W375.
17. Koradi, R.; Billeter, M.; Wüthrich, K. *J Mol Graph.* **14**, 51. (1996).
18. Jee, J. G.; Ikegami, T.; Hashimoto, M.; Kawabata, T.; Ikeguchi, M.; Watanabe, T.; Shirakawa, M. *The Journal of biological chemistry.* **277**, 1388. (2002).
19. Mongan, J.; Simmerling, C.; McCammon, J. A.; Case, D. A.; Onufriev, A. *Journal of chemical theory and computation.* **3**, 156. (2007).
20. Lim, J.; Ahn, H.-C. *J Kor Mag Res Soc.* **16**, 46. (2012).
21. Sim, D.-W.; Jo, K.-S.; Ryu, K.-S.; Kim, E.-H.; Won, H.-S. *J Kor Mag Res Soc.* **16**, 21. (2012).